

NASA Technical Memorandum 79302

A TIME DEPENDENT DIFFERENCE THEORY
FOR SOUND PROPAGATION
IN DUCTS WITH FLOW

(NASA-TM-79302) A TIME DEPENDENT DIFFERENCE
THEORY FOR SOUND PROPAGATION IN DUCTS WITH
FLOW (NASA) 38 p HC A03/MF A01 CSCL 20A

N80-12823

Unclas
G3/71 46206

K. J. Baumeister
Lewis Research Center
Cleveland, Ohio



Prepared for the
Ninety-eighth Meeting of the Acoustical Society of America
Salt Lake City, Utah, November 26-30, 1979

A TIME DEPENDENT DIFFERENCE THEORY
FOR SOUND PROPAGATION IN DUCTS WITH FLOW

K. J. Baumeister

NASA Lewis Research Center
Cleveland, Ohio

ABSTRACT.

E-254 A time dependent numerical solution of the linearized continuity and momentum equation is developed for sound propagation in a two-dimensional straight hard or soft wall duct with a sheared mean flow. The time dependent governing acoustic-difference equations and boundary conditions are developed along with a numerical determination of the maximum stable time increments. The analysis begins with a harmonic noise source radiating into a quiescent duct. This explicit iteration method then calculates stepwise in real time to obtain the transient as well as the "steady" state solution of the acoustic field. Example calculations are presented for sound propagation in hard and soft wall ducts, with no flow and with plug flow. Although the problem with sheared flow has been formulated and programmed, sample calculations have not yet been examined. So far, the time dependent finite difference analysis has been found to be superior to the steady state finite difference and finite element techniques because of shorter solution times and the elimination of large matrix storage requirements.

List of Symbols

c_0^*	ambient speed of sound, m/s
f^*	frequency, Hz
H^*	duct height, m
I	number of axial grid points
i	$\sqrt{-1}$
J	number of transverse grid points
k	number of time steps
L^*	length of duct, m
M	Mach number $M(y)$, U^*/c_0^*
n	transverse mode number
P	time dependent acoustic pressure, $P^*/\rho^* c_0^{*2}$
p	spatially dependent acoustic pressure
P_S	spatially dependent solution of Wave Equation
T^*	period, $1/f^*$, sec
t	dimensionless time, t^*/T^*
Δt	time step
U^*	mean flow velocity $U^*(y^*)$, m/sec
u	axial acoustic velocity, u^*/c_0^*
v	transverse acoustic velocity, v^*/c_0^*
x	axial coordinate, x^*/H^*
Δx	axial grid spacing
y	dimensionless transverse coordinate, y^*/H^*
Δy	transverse grid spacing

Z^*	impedance, $\text{kg/m}^2\text{sec}$
α	stability factor, eq. (29)
ζ	specific acoustic impedance
η	dimensionless frequency, H^*f^*/c_0^*
θ	dimensionless resistance
ρ_0^*	ambient air density, kg/m^3
χ	dimensionless reactance
ω	angular frequency

Subscripts

c	calculation, time
e	exit condition
i	axial index (Fig. 1)
j	transverse index (Fig. 1)
o	ambient condition
s	spatial value
t	transient

Superscripts

*	dimensional quantity
k	time step index
(1)	real part
(2)	imaginary part

INTRODUCTION

Both finite difference and finite element numerical techniques (refs. 1 to 27) have been developed to study sound propagation with axial variations in Mach number, wall impedance, and duct geometry as might be encountered in a typical turbojet engine. Generally, the numerical solutions have been limited to low frequency sound and short ducts, because many grid points or elements were required to resolve the axial wavelength of the sound. As shown in reference 1 (eq. (77)) for plane wave propagation, the number of axial grid points or elements is directly proportional to the sound frequency and duct length, and inversely proportional to the difference of unity minus the Mach number (ref. 2). This latter dependence also severely limits the application of numerical techniques for high Mach number inlets.

Customarily, the pressure and acoustic velocities are assumed to be simple harmonic functions of time; thus, the governing linearized gas-dynamic equations (ref. 28, pg. 5) become independent of time. The matrices associated with the numerical solution to the time independent equations must be solved exactly using such methods as Gauss elimination. As a result, large arrays of matrix elements must be stored which tax the storage capacity of even the largest computer. In an unpublished work at NASA Lewis Research Center by the author using reference 29, as well as in the work of Quinn (ref. 23, pg. 3), the matrix has been modified to allow iteration techniques; unfortunately, the convergence is too slow to be of any practical value.

Other approaches, such as in reference 30, might still offer iterative possibilities.

Some special techniques have been developed to overcome the difficulties of low frequency, short ducts, and low Mach numbers. As shown in references 3 and 10, the wave envelope numerical technique can reduce the required number of grid points by an order of magnitude. In reference 20, this technique was used to optimize multi-element liners of long lengths at high frequencies. At the present time, this technique has been applied only to the simple cases of no flow and plug flow. A numerical spatial marching technique was also developed in references 15 and 18. Compared to the standard finite difference or finite element boundary value approaches, the numerical marching technique is orders of magnitude shorter in computational time and required computer storage. The marching technique is limited to high frequencies and to cases where reflections are small.

As an alternative to the previously developed steady state theories, a time dependent numerical solution is developed herein for noise propagation in a two-dimensional soft wall duct with parallel sheared mean flow. Advantageously, matrix storage requirements are significantly reduced in the time dependent analysis. The analysis begins with a noise source radiating into an initially quiescent duct. This explicit method calculates stepwise in real time to obtain the transient as well as the "steady" state solution of the acoustic field. The total time required for the analysis to calculate the "steady" state acoustic field

will determine the usefulness of the time dependent technique.

Time dependent numerical techniques have been applied extensively to one-dimensional sound propagation (ref. 31, pg. 258 and ref. 32), two-dimensional vibration problems (ref. 33, pg. 452) and the more general problem of compressible fluid flow (ref. 34). References 35 and 36 discuss in detail the stability of time dependent numerical solutions.

In a companion paper to this work (ref. 37), the explicit time iteration techniques of references 31 to 36 are extended to include soft-wall impedance boundary conditions which would be encountered in inlets and exhaust ducts of turbo-fan jet engines. The analysis applies to two-dimensional straight hard and soft wall ducts without flow. In the absence of mean flow, the governing acoustic equation was the classic second order wave equation. The time dependent solution to the wave equation was found to be superior to the conventional steady numerical analysis because of much shorter solution times and the elimination of large matrix storage requirements.

When parallel shear flow occurs in a duct, the second order formulation of reference 37 cannot be used since the governing differential wave equation is third order (ref. 28, pg. 9). Rather than attempt to solve a third order wave equation, in the present paper the first order equations of continuity and momentum will be solved simultaneously. First, the governing acoustic equations and boundary conditions

are presented for time dependent propagation in a parallel sheared mean flow. Next, the governing acoustic-difference equations and boundary conditions are derived. The two-dimensional stability theory is then used as a guide to estimate the maximum stable time increment. Immediately following the mathematical development, numerical solutions are presented for one-and-two-dimensional hard and soft-wall ducts. The results are compared with the corresponding steady state analytical results. Finally, the times required to perform both the time dependent and steady state analyses are compared for increasing number of grid points.

1. GOVERNING EQUATIONS AND BOUNDARY CONDITIONS

The propagation of sound in a two-dimensional rectangular duct, shown in Figure 1, is described by the linearized continuity and momentum equations and the appropriate impedance boundary conditions.

A. Continuity and Momentum

The linearized equations for mass and momentum conservation (ref. 28, pg. 5) can be written for a Cartesian coordinate system in the following dimensionless form:

continuity

$$\frac{\partial P}{\partial t} = -\frac{1}{\eta} \frac{\partial u}{\partial x} - \frac{1}{\eta} \frac{\partial v}{\partial y} - \frac{M}{\eta} \frac{\partial P}{\partial x} \quad (1)$$

x-momentum

$$\frac{\partial u}{\partial t} = -\frac{1}{\eta} \frac{\partial P}{\partial x} - \frac{M}{\eta} \frac{\partial u}{\partial x} - \frac{1}{\eta} \frac{\partial M}{\partial y} v \quad (2)$$

y-momentum

$$\frac{\partial v}{\partial t} = -\frac{1}{\eta} \frac{\partial P}{\partial y} - \frac{M}{\eta} \frac{\partial v}{\partial x} \quad (3)$$

These and other symbols are defined in the Nomenclature. The dimensionless frequency η is defined as:

$$\eta = \frac{H^*}{2\pi} \frac{\omega^*}{c_0^*} = \frac{H^* f^*}{c_0^*} \quad (4)$$

The asterisks define dimensional quantities.

The foregoing dimensionless equations apply to the scaled Cartesian coordinate system in which the dimensionless height (y^*/H^*) ranges between 0 and 1 and the dimensionless length ranges between 0 and L^*/H^* .

B. Wall Boundary Conditions

The boundary condition on the transverse acoustic velocity v at the surface of a sound absorbent soft-wall duct can be expressed in terms of a specific acoustic impedance ζ

$$v(x, l, t) = \frac{P(x, l, t)}{\zeta} \quad (5)$$

where the complex specific wall impedance is defined as

$$\zeta = \frac{Z^*}{\rho_o^* c_o^*} = \theta + i\chi \quad (6)$$

At the lower wall, the sign on ζ is changed to account for the vector nature of v .

In addition to equation (5), another form of the wall impedance condition will be considered. Substituting equation (5) into equation (3), noting that the Mach number is zero at the wall, and assuming ζ is a constant independent of time, then

$$\frac{\partial P}{\partial y} = -\frac{\eta}{\zeta} \frac{\partial P}{\partial t} \quad (7)$$

This form of the impedance boundary condition cannot be used for plug flow when a soft wall is present.

C. Entrance Condition

The boundary condition at the source plane $P(o, y, t)$ can be of any general form with both transverse variations in pressure and multiple

frequency content. However, the numerical technique will be compared later to previous solutions in which the pressure and acoustic velocities were assumed to be plane waves at the entrance and to vary as $e^{i\omega^*t^*}$ or in dimensionless form as $e^{i2\pi t}$. Therefore, the source boundary condition used here is

$$P(0, y, t) = e^{i2\pi t} \quad (8)$$

D. Exit Impedance

In a manner similar to the wall impedance, the axial acoustic velocity at the duct exit can be expressed in terms of a specific acoustic exit impedance ζ_e as

$$u(L^*/H^*, y, t) = \frac{P(L^*/H^*, y, t)}{\zeta_e} \quad (9)$$

For the plane wave propagation to be considered herein, ζ_e is taken to be equal to unity, which is exact for plane wave propagation in an infinite hard-wall duct. Also, choosing ζ_e to be equal to unity has led to close agreement between numerical and analytical results for plane wave propagation into a soft-wall duct (refs. 1 and 3). More general values for the exit impedance can be found in references 7, 15 (eq. B-4), 16, or 18 (fig. 7).

E. Initial Conditions

For times equal to or less than zero, the duct is assumed quiescent; that is, the acoustic pressure and velocities are taken to be zero. For

times greater than zero, the application of the noise source, equation (8), will drive the pressures in the duct.

F. Complex Notation

Because of the introduction of complex notation for the noise source and wall impedance, all the dependent variables are complex. The superscript (1) will represent the real term while (2) will represent the imaginary term

$$p = p^{(1)} + ip^{(2)} \tag{10}$$

A similar notation applies to the acoustic velocities.

II. DIFFERENCE EQUATIONS

Instead of a continuous solution for pressure in space and time, the finite difference approximations will determine the pressure at isolated grid points in space as shown in Figure 1 and at discrete time steps Δt . Starting from the known initial conditions at $t=0$ and the boundary conditions, the finite difference algorithm will march-out the solution to later times.

A. Central Region

Away from the duct boundaries of Figure 1, the derivatives in the governing equations can be represented by the following differences in time and space:

$$\frac{P_{i,j}^{k+1} - P_{i,j}^k}{\Delta t} = -\frac{1}{\eta} \left(\frac{u_{i+1,j}^k - u_{i-1,j}^k}{2\Delta x} \right) - \frac{1}{\eta} \left(\frac{v_{i,j+1}^k - v_{i,j-1}^k}{2\Delta y} \right) \quad (11)$$

$$\begin{aligned} & -\frac{M}{\eta} \left(\frac{P_{i+1,j}^k - P_{i-1,j}^k}{2\Delta x} \right) \\ \frac{u_{i,j}^{k+1} - u_{i,j}^k}{\Delta t} &= -\frac{1}{\eta} \left(\frac{P_{i+1,j}^{k+1} - P_{i-1,j}^{k+1}}{2\Delta x} \right) - \frac{M}{\eta} \left(\frac{u_{i+1,j}^k - u_{i-1,j}^k}{2\Delta x} \right) \quad (12) \\ & -\frac{v_{i,j}^k}{\eta} \frac{\partial M}{\partial y} \end{aligned}$$

$$\frac{v_{i,j}^{k+1} - v_{i,j}^k}{\Delta t} = -\frac{1}{\eta} \left(\frac{p_{i,j+1}^{k+1} - p_{i,j-1}^{k+1}}{2\Delta y} \right) - \frac{M}{\eta} \left(\frac{v_{i+1,j}^k - v_{i-1,j}^k}{2\Delta x} \right) \quad (13)$$

where i and j denote the space indices, k the time index and Δx , Δy , Δt are the space and time mesh spacing respectively. All spacings are assumed constant. The time is defined as

$$t^{k+1} = t^k + \Delta t = (k+1)\Delta t \quad (14)$$

Solving equations (11), (12), and (13) for the acoustic pressures and velocities yields

continuity

$$p_{i,j}^{k+1} = p_{i,j}^k - \frac{1}{2\eta} \frac{\Delta t}{\Delta x} \left(u_{i+1,j}^k - u_{i-1,j}^k \right) - \frac{1}{2\eta} \frac{\Delta t}{\Delta y} \left(v_{i,j+1}^k - v_{i,j-1}^k \right) - \frac{M}{2\eta} \frac{\Delta t}{\Delta x} \left(p_{i+1,j}^k - p_{i-1,j}^k \right) \quad (15)$$

x-momentum

$$u_{i,j}^{k+1} = u_{i,j}^k - \frac{1}{2\eta} \frac{\Delta t}{\Delta x} \left(p_{i+1,j}^{k+1} - p_{i-1,j}^{k+1} \right) - \frac{M}{2\eta} \frac{\Delta t}{\Delta x} \left(u_{i+1,j}^k - u_{i-1,j}^k \right) - \frac{\Delta t}{\eta} \frac{\partial M}{\partial y} v_{i,j}^k \quad (16)$$

y-momentum

$$v_{i,j}^{k+1} = v_{i,j}^k - \frac{\Delta t}{2\eta\Delta y} \left(P_{i,j+1}^{k+1} - P_{i,j-1}^{k+1} \right) - \frac{M}{2\eta} \frac{\Delta t}{\Delta x} \left(v_{i+1,j}^k - v_{i-1,j}^k \right) \quad (17)$$

Equations (15), (16), and (17) are algorithms which permit marching out solutions from known values of pressure and velocities at times associated with k and $k-1$. First, equation (15) is solved for P^{k+1} at all grid points prior to solving equations (16) and (17). In this manner, new values of P^{k+1} are available for use in equations (16) and (17). The procedure is explicit since all the past values of P^k are known as the new values of P^{k+1} are computed. For the special case at $t=0$, the values of the pressure and velocities associated with the $k-1$ value are zero from the assumed initial conditions.

B. Wall Condition

Recall that at the wall, the transverse velocity is governed by the wall impedance as given by equation (5). Therefore, at the wall, the y-momentum equation (17) was initially replaced by the difference form of equation (5) which in this case is

$$v_{i,j}^{k+1} = P_{i,j}^{k+1}/\zeta \quad (18)$$

Thus, equations (15), (16), and (18) are the governing equations at the wall.

The numerical solutions remained stable in the example problems involving hard-wall ducts ($\zeta = \infty$). Unfortunately, in the soft-wall example

problems considered, the numerical procedure went unstable. Introducing equation (18) appears to lead to an instability for finite values of ζ . An explanation of why this went unstable will be presented later in the section which discusses the stability of the difference equations. In the meantime, the following new wall boundary condition is developed to replace equation (18).

Associated with the new wall boundary condition, the grid structure shown in Figure 2 is used to establish the pressure gradient at the wall boundary which satisfies the impedance condition. Equation (7) can be written in difference form as

$$\frac{P_{i,j}^{k+1} - P_{k,j}^k}{\Delta t} = -\frac{\zeta}{\eta} \left(\frac{P_{i,j}^{k+1} - P_{i,j-1}^{k+1}}{\Delta y} \right) \quad (19)$$

Notice that the values of pressure gradient are expressed in the new values of pressure. This can be extremely important in stability considerations, as will be discussed later. The value of $P_{i,j}^{k+1}$ are first found in the central points away from the boundary; consequently, $P_{1,j-1}^{k+1}$ is a known value in equation (19). Solving for the acoustic pressure at the wall yields ($j = J$)

$$P_{i,j}^{k+1} = \frac{P_{i,j-1}^{k+1} + \frac{\eta}{\zeta} \frac{\Delta y}{\Delta t} P_{i,j}^k}{\left(1 + \frac{\eta \Delta y}{\zeta \Delta t}\right)} \quad (20)$$

A similar equation applies at the lower wall.

Equations (20) and (18) now determine the pressure and velocity in the wall. The pressures and transverse velocities at the wall would be the average of their values at the grid points which straddle the wall. The calculation of the axial velocities at the wall grid point is not yet required. The axial velocity at the wall will be the value associated with the point J-1.

C. Entrance Condition

At the entrance conditions, the continuity equation is replaced by equation (8) and the difference form of the momentum equations must be expressed in terms of forward differences. In this case, the governing difference equations become

$$P_{1,j}^{k+1} = e^{i2\pi(k+1)\Delta t} \quad t > 0 \quad (21)$$

$$u_{1,j}^{k+1} = u_{1,j}^k - \frac{\Delta t}{\eta\Delta x} \left(P_{2,j}^{k+1} - P_{1,j}^{k+1} \right) - \frac{M\Delta t}{\eta\Delta x} \left(u_{2,j}^k - u_{1,j}^k \right) - \frac{\partial M}{\partial y} \frac{\Delta t}{\eta} v_{1,j}^k \quad (22)$$

$$v_{1,j}^{k+1} = v_{1,j}^k - \frac{\Delta t}{2\eta\Delta y} \left(P_{1,j+1}^{k+1} - P_{1,j-1}^{k+1} \right) - \frac{M\Delta t}{\eta\Delta x} \left(v_{2,j}^k - v_{1,j}^k \right) \quad (23)$$

D. Exit Condition

Similarly to the entrance condition, the governing equations must be expressed in terms of the backward differences. In this case, the governing difference equations become ($i = 1$)

$$P_{i,j}^{k+1} = P_{i,j}^k - \frac{\Delta t}{\eta\Delta x} \left(u_{i,j}^k - u_{i-1,j}^k \right) - \frac{\Delta t}{2\eta\Delta y} \left(v_{i,j+1}^k - v_{i,j-1}^k \right) - \frac{M\Delta t}{\eta\Delta x} \left(P_{i,j}^k - P_{i-1,j}^k \right) \quad (24)$$

$$u_{i,j}^{k+1} = P_{i,j}^{k+1} / \zeta_e \quad (25)$$

$$v_{i,j}^{k+1} = v_{i,j}^k - \frac{\Delta t}{2\eta\Delta y} \left(P_{i,j+1}^{k+1} - P_{i,j-1}^{k+1} \right) - \frac{M\Delta t}{\eta\Delta x} \left(v_{i,j}^k - v_{i-1,j}^k \right) \quad (26)$$

E. Spatial Mesh Size

The mesh spacing Δx and Δy must be restricted to small values to reduce the truncation error. To resolve the oscillatory nature of the pressure, the required number of grid points in the axial direction suggested is (see ref. 1)

$$I \geq \frac{12\eta L^* / H^*}{(1 + M)} \quad (27)$$

while the number of points in the transverse direction suggested in reference 37 is

$$J \geq 12\eta \quad (28)$$

III. STABILITY

In the explicit time marching approach used here, round-off errors can grow in an unbounded fashion and destroy the solution if the difference equation is improperly formulated or the time increment Δt is taken too large. Although at least six methods (ref. 34, pg. 48) of stability analysis exist, none are entirely adequate when obtaining actual solutions to differential equations (ref. 34, pg. 51). Consequently, numerical experimentation will be used to determine the actual stability. The simpler stability analyses will be used to guide the development of the difference form of the governing equations and the choice of the time increments.

Using the two-dimensional (space and time) no flow stability analysis of Courant, Friedrichs and Lewy (ref. 31, pg. 262) as a guide, p^{k+1} values were used in equations (12) and (13) instead of P^k . If the values of P at P^k instead of at P^{k+1} had been used in equations (12) and (13), the iteration scheme would be unstable. To avoid instabilities, as a general rule, the new values of the dependent variables will be used whenever possible (see equation (19), for example).

The stability requirement for the no flow situation suggested in reference 37 is

$$\alpha = \frac{\Delta t^2}{\eta^2 \Delta y^2} \left[1 + \left(\frac{\Delta y}{\Delta x} \right)^2 \right] < 1 \quad (29)$$

which limits the time increment to

$$\Delta t \leq \frac{\eta \Delta y}{\sqrt{1 + (\Delta y / \Delta x)^2}} \quad (30)$$

To account for Mach number, equation (30) is empirically modified to

$$\Delta t \leq \frac{\eta \Delta y (1 - |M|)}{\sqrt{1 + (\Delta y / \Delta x)^2}} \quad (31)$$

where the largest value of the local Mach number is used. Equation (31) is used to set the initial time increment. If an instability should occur, the time increment will be reduced until stability occurs.

IV. STEADY STATE PRESSURES

In the sample problems to be presented in the next section, the time dependent results will be compared to the results of the steady harmonic solutions of reference 10. The purpose of this section is to show the rationale for constructing a steady state solution from the time dependent results.

A. Steady Harmonic Solution

The steady harmonic pressure $p_s(x,y)$ is defined as a solution to equations (1) to (3) when the pressure is assumed to be a simple harmonic function of time:

$$P(x,y,t) = p_s(x,y)e^{i2\pi t} \quad (32)$$

In this case where the source is a simple harmonic function of time, p_s represents the Fourier transform of $p(x,y,t)$ (ref. 28, pg. 11).

For a semi-infinite duct (or an equivalent finite duct with a $\rho^* c_o^*$ exit impedance) with plane wave propagation, uniform Mach number, and hard walls, the solution for p_s is (ref. 10, eq. (18))

$$p_s = e^{\frac{-i2\pi x}{(1+M)}} \quad (33)$$

In the next section, a transient solution to this problem will be compared to equation (33).

B. Transient Times

Recall, at the start of the numerical calculations, the acoustic pressures and velocities were assumed zero throughout the duct. Then, a pressure source begins a harmonic oscillation at $x=0$ for t greater than zero. For the special case of a plane wave propagation without flow in a hard wall semi-infinite duct, the analytical solution to the wave equation indicates that the transient solution ends and the steady solution p_s begins when (ref. 38, pg. 305)

$$t_t > \eta x \quad (34)$$

or in terms of real variable when

$$t_t^* > x^*/c_0^* \quad (35)$$

The transient time in equations (34) and (35) represents the time for the wave to travel down to the end of the duct, $x^* = L^*$.

The transient time can be shortened or expanded depending on the direction of the flow and the transverse velocity distribution. In general, the length of time for the transient to occur will be found by a trial numerical procedure. For the simple case of plug flow, equation (34) is now modified to include a uniform Mach number.

$$t_t > \frac{\eta x}{1 + M} \quad (36)$$

Therefore, for the special case of one-dimensional plane wave propagation, the initial transient is assumed to pass when equation (36) holds. As a

factor of safety in the present calculations, the transient calculation will be continued into the steady domain for one period of oscillation before the Fourier pressure p is calculated. Therefore, in this paper

$$t_c = \frac{\eta L^*/H^*}{(1 + M)} + 1 \quad (37)$$

and

$$p(x,y) = \frac{P(x,y,t)}{e^{i2\pi t_c}} \quad (38)$$

For more complicated problems, such as with higher order modes, where reflections are important, or where complicated flow gradients exist, t_c should be increased in successive steps to check for convergence.

V. SAMPLE CALCULATIONS

In the sample problems to follow, the time dependent results will be compared to the analytical results of equation (33) and the steady harmonic numerical solutions of reference (10).

A. Hard-Wall Duct

Numerical and analytical values of the pressure $p(x,y)$ are computed for the case of a hard-wall duct for plane wave propagation with $\zeta_e = 1$ exit impedance (equivalent to a semi-infinite duct) for no flow and plug flow with Mach numbers of -0.5 and $+0.5$. The calculations are made with a length to height ratio (L^*/H^*) of 1 and a dimensionless frequency η of 1. The analytical and numerical values of the acoustic pressure profiles along the duct are shown in Figures 3, 4, and 5. As seen in these figures, the agreement between the analytical and numerical theory is reasonably good.

Some inaccuracy exists in the pressure at the entrance ($x = 0$). As seen in Figures 3 and 4, the pressure at the second grid location takes a slight jump. This is believed to result because the approximations for the spatial derivatives are only first order at the corners. Future work should be concerned with developing higher order difference approximations which are more accurate and stable. Higher order difference would also be desirable in order to increase the mesh spacing used in these calculations, and thereby reduce the number of grid points.

B. Soft-Wall Ducts

As another example of the time dependent analysis, the pressure distribution was computed for the case of plane wave propagation without steady flow and with a $\zeta_e = 1$ exit impedance and a wall with impedance value of $0.16 - i 0.34$. The calculation was made with a length to height ratio of 0.5 and a dimensionless frequency of 0.6. The results of the time dependent analysis along with the results of the solution of the equivalent steady state Helmholtz equation are displayed in Figure 6. The numerical results for the steady spatial solution $p_s(x,y)$ are tabulated in Appendix F of reference 10.

Again, as seen in Figure 6, the steady state and time dependent solutions are in reasonable agreement. Hopefully, the difference between both theories can be resolved by using higher order difference approximations.

C. Grid Point Variations

Figure 7 shows the effect of increasing the number of grid points on the computational time of the time dependent approach for the hard wall duct associated with Figure 3. Roughly, as seen in Figure 4, the computational time is proportional to the number of grid points used. This is considerable advantage over the steady state technique in which the computational time more nearly increases with the square of the total grid points.

Figure 8 shows a comparison of the computational times for the steady state and time dependent problems associated with the hard wall duct shown in Figure 2. For this no-flow example, the continuity and momentum equations, (1) to (3), can be combined into a single wave equation

$$\eta^2 \frac{\partial^2 P}{\partial t^2} = \frac{\partial^2 P}{\partial x^2} + \frac{\partial^2 P}{\partial y^2} \quad (39)$$

The time dependent solution to equation (39) was presented in reference 37 and is represented by the lowest line in Figure 8.

As seen in Figure 8 for $J = 20$, the time dependent analysis presented herein is roughly equal to the steady state analysis. The value of J (grid points in y -direction) was restricted to 20 because of practical limitations on the size of the matrix which could be effectively handled in the steady state analysis. When J was increased to 50 with 50 axial grid points, the steady state analysis required 5500 seconds as compared to less than 150 seconds for the time dependent analysis. This large increase in the steady state solution time results because of the manner in which the general matrix was partitioned (ref. 10, pg. 14). In this case, the storage and computational times are proportional to the total number of transverse grid points squared.

As seen in Figure 8, the time dependent solutions for the continuity and momentum formulation in this paper require computational times a factor of 10 greater than the transient solution times to the wave equation

for the same degree of accuracy. This results because much smaller time increments Δt must be taken with the continuity and momentum solutions to obtain the same accuracy or truncation error. In the numerical formulation of the wave equation (eq. (39)), the second derivative of time is expressed in terms of the usual central difference approximation:

$$\frac{\partial^2 p}{\partial t^2} = \frac{p_{i,j}^{k+1} - 2p_{i,j}^k + p_{i,j}^{k-1}}{\Delta t^2} + o(\Delta t^2) \quad (40)$$

where the truncation error is of order Δt^2 . On the other hand, in the continuity equation (eq. (11)), the first derivative of time is expressed as a forward difference

$$\frac{\partial p}{\partial t} = \frac{p_{i,j}^{k+1} - p_{i,j}^k}{\Delta t} + o(\Delta t) \quad (41)$$

where the truncation error is of order Δt . Consequently, a numerical solution based on equation (41) will require smaller time steps for the same degree of accuracy.

D. Shear Flow

Although the shear flow difference equations have been programmed, at the present time shear flow example problems have not been examined.

CONCLUSIONS

A time dependent two-dimensional explicit numerical procedure was developed for the parallel sheared mean flow form of the separate continuity and momentum equations. This time marching technique was found to be stable for both no flow and plug flow. At the present time, shear flow examples have not been attempted. A special wall boundary condition was developed to insure stability for the soft wall case.

With the possible exception of the wave envelope technique (ref. 10) or the spatial marching technique (ref. 18), the numerical time dependent method of analysis represents a significant advance over previous steady numerical theories. By eliminating large matrix storage requirements, numerical calculations of high sound frequencies are now possible. Because manipulation of matrices is omitted, the time dependent approach is much easier to program and debug.

REFERENCES

1. K. J. Baumeister and E. C. Bittner, "Numerical Simulation of Noise Propagation in Jet Engine Ducts," NASA TN D-7339 (1973).
2. K. J. Baumeister and E. J. Rice, "A Difference Theory for Noise Propagation in an Acoustically Lined Duct with Mean Flow," in Aeroacoustics: Jet and Combustion Noise; Duct Acoustics, edited by H. T. Nagamatsu, J. V. O'Keefe, and I. R. Schwartz, Progress in Astronautics and Aeronautics Series, Vol 37 (American Institute of Aeronautics and Astronautics, New York, 1975), pp. 435-453.
3. K. J. Baumeister, "Analysis of Sound Propagation in Ducts Using the Wave Envelope Concept," NASA TN D-7719 (1974).
4. D. W. Quinn, "A Finite Difference Method for Computing Sound Propagation in Nonuniform Ducts," AIAA Paper No. 75-130 (January 1975).
5. K. J. Baumeister, "Wave Envelope Analysis of Sound Propagation in Ducts with Variable Axial Impedance," in Aeroacoustics: Duct Acoustics, Fan Noise and Control Rotor Noise, edited by I. R. Schwartz, H. T. Nagamatsu, and W. Strahle, Progress in Astronautics and Aeronautics Series, Vol. 44 (American Institute of Aeronautics and Astronautics, New York, 1976), pp. 451-474.
6. D. W. Quinn, "Attenuation of Sound Associated with a Plane Wave in a Multisectional Duct," in Aeroacoustics: Duct Acoustics, Fan Noise and Control Rotor Noise, edited by I. R. Schwartz, H. T. Nagamatsu, and W. Strahle, Progress in Astronautics and Aeronautics Series, Vol. 44 (American Institute of Aeronautics and Astronautics, New York, 1976), pp. 331-345.

7. R. K. Sigman, R. K. Majjigi, and B. T. Zinn, "Determination of Turbofan Inlet Acoustics using Finite Elements," AIAA 16, pp. 1139-1145 (1978).
8. A. L. Abrahamson, "A Finite Element Algorithm for Sound Propagation in Axisymmetric Ducts Containing Compressible Mean Flow," NASA CR-145209 (June 1977).
9. A. Craggs, "A Finite Method for Modelling Dissipative Mufflers With a Locally Reactive Lining," Sound Vib. 54, pp. 285-296 (1977).
10. K. J. Baumeister, "Finite-Difference Theory for Sound Propagation in a Lined Duct with Uniform Flow Using the Wave Envelope Concept," NASA TP-1001 (1977).
11. Y. Kagawa, T. Yamabuchi, and A. Mori, "Finite Element Simulation of an Axisymmetric Acoustic Transmission System with a Sound Absorbing Wall," Sound Vib. 53, pp. 357-374 (1977).
12. W. Eversman, R. J. Astley, and V. P. Thanh, "Transmission in Non-uniform Ducts - A Comparative Evaluation of Finite Element and Weighted Residuals Computational Schemes," AIAA Paper No. 77-1299 (October 1977).
13. R. Watson, "A Finite Element Simulation of Sound Attenuation in a Finite Duct With a Peripherally Variable Liner," AIAA Paper No. 77-1300 (October 1977).
14. A. L. Abrahamson, "A Finite Element Algorithm for Sound Propagation in Axisymmetric Ducts Containing Compressible Mean Flow," AIAA Paper No. 77-1301 (October 1977).

15. K. J. Baumeister, "Numerical Spatial Marching Techniques for Estimating Duct Attenuation and Source Pressure Profiles," in 95th Meeting of the Acoustical Society of America, Providence, R.I., (May 16-19, 1978), also published as NASA TM-78857 (1978).
16. I. A. Tag and E. Lumsdaine, "An Efficient Finite Element Technique for Sound Propagation in Axisymmetric Hard Wall Ducts Carrying High Subsonic Mach Number Flows," AIAA Paper No. 78-1154 (July 1978).
17. R. J. Astley and W. Eversman, "A Finite Element Method for Transmission in Non-Uniform Ducts without Flow: Comparison with the Method of Weighted Residuals," Sound Vib. 57, pp. 367-388 (1978).
18. K. J. Baumeister, "Numerical Spatial Marching Techniques in Duct Acoustics," J. Acoust. Soc. Am. 65, pp. 297-306 (1979).
19. R. K. Majjigi, "Application of Finite Element Techniques in Predicting the Acoustic Properties of Turbofan Inlets," Ph. D. Thesis, Georgia Institute of Technology, Atlanta, GA, (1979).
20. K. J. Baumeister, "Optimized Multisectioned Acoustic Liners," AIAA Paper No. 79-0182 (January 1979).
21. R. K. Majjigi, R. K. Sigman, and B. T. Zinn, "Wave Propagation in Ducts Using the Finite Element Method," AIAA Paper No. 79-0659 (March 1979).
22. R. J. Astley and W. Eversman, "The Application of Finite Element Techniques to Acoustic Transmission in Lined Ducts with Flow," AIAA Paper No. 79-0660 (March 1979).
23. D. W. Quinn, "A Finite Element Method for Computing Sound Propagation in Ducts Containing Flow," AIAA Paper No. 79-0661 (March 1979).

24. A. L. Abrahamson, "Acoustic Duct Liner Optimization Using Finite Elements," AIAA Paper No. 79-0662 (March 1979).
25. I. A. Tag and J. E. Akin, "Finite Element Solution of Sound Propagation in a Variable Area Duct," AIAA Paper No. 79-0663 (March 1979).
26. H. C. Lester and T. L. Parrott, "Application of Finite Element Methodology for Computing Grazing Incidence Wave Structure in an Impedance Tube: Comparison with Experiment," AIAA Paper No. 79-0664 (March 1979).
27. K. J. Baumeister and R. K. Majjigi, "Applications of the Velocity Potential Function to Acoustic Duct Propagation and Radiation from Inlets Using Finite Element Theory," AIAA Paper No. 79-0680 (March 1979).
28. M. E. Goldstein, Aeroacoustics, (McGraw-Hill, New York, 1976).
29. M. J. Beaubien and A. Wexler, "Iterative, Finite Difference Solution of Interior Eigenvalues and Eigenfunctions of Laplace's Operator," *The Computer J.* 14, pp. 263-269 (1971).
30. B. T. Browne and P. J. Lawrenson, "Numerical Solution of an Elliptic Boundary-Value Problem in the Complex Variable," *J. Inst. Maths. Applics.* 17, pp. 311-327 (1976).
31. R. D. Richtmyer and K. W. Morton, Difference Methods for Initial-Value Problems, (Interscience Publishers, New York, 1967), 2nd ed.
32. P. Fox, "The Solution of Hyperbolic Partial Differential Equations by Difference Methods," in Mathematical Methods for Digital Computers, edited by A. Ralston and H. S. Wilf (John Wiley, New York, 1960), Vol. 1, pp. 180-188.

33. C. F. Gerald, Applied Numerical Analysis, (Addison-Wesley, Reading, MA, 1978), 2nd ed.
34. P. J. Roache, Computational Fluid Dynamics, (Hermosa, Albuquerque, N. M., 1972).
35. M. Clark and K. F. Hansen, Numerical Methods of Reactor Analysis, (Academic Press, New York, 1964).
36. F. B. Hildebrand, Methods of Applied Mathematics, (Prentice-Hall, New Jersey, 1952).
37. K. J. Baumeister, "Time Dependent Difference Theory for Noise Propagation in Jet Engine Ducts," AIAA Paper No. 80-0098, to be presented AIAA 18th Aerospace Sciences Meeting, Pasadena, CA, (January 14-16, 1980).
38. B. M. Budak; A. A. Samarski, and A. N. Tikhonov, A Collection of Problems on Mathematical Physics, (Pergamon Press, Oxford, 1964).

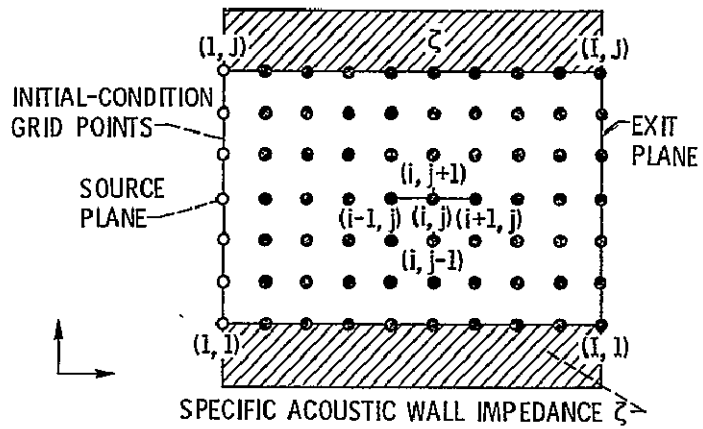


Figure 1. - Grid-point representation of two-dimensional flow duct

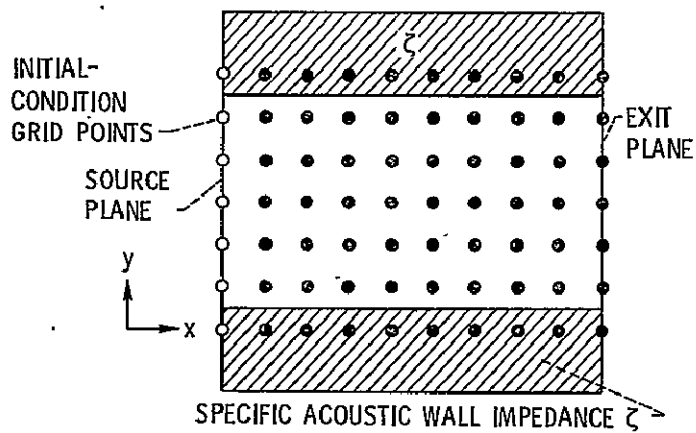


Figure 2. - Grid-point representation of two-dimensional flow duct using pressure boundary condition at walls.

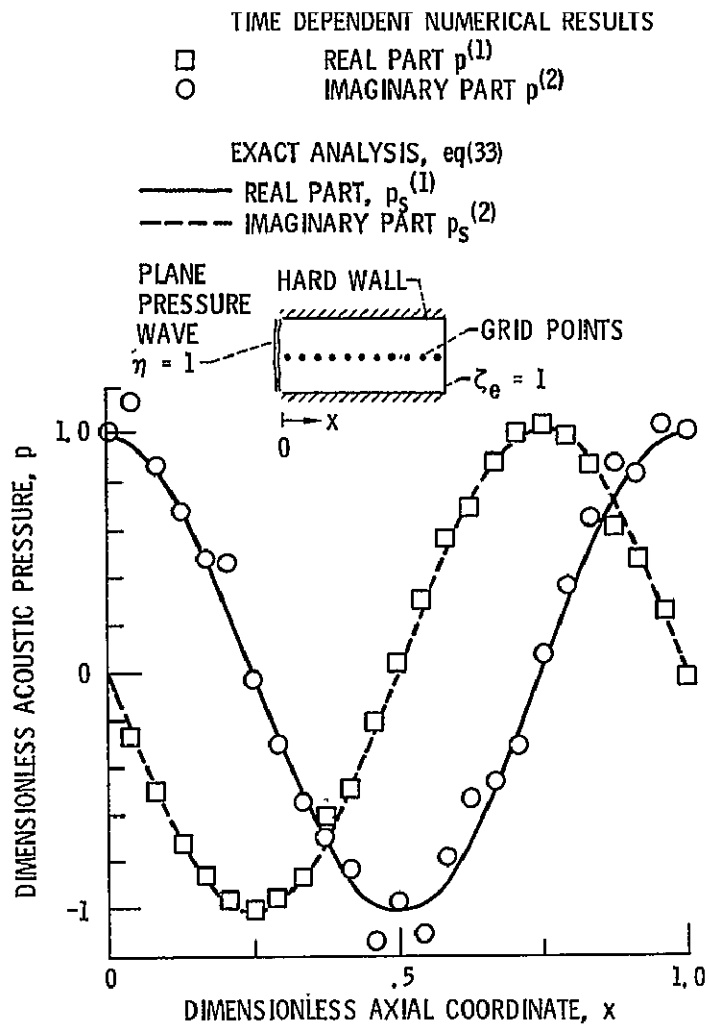


Figure 3 - Analytical and numerical pressure profiles for one-dimensional plane wave sound propagation in a hard wall duct for $M=0$, $\eta = 1$, and $L^*/H^* = 1$ ($I = 25$, $J = 20$, $\Delta t = 0.004084$).

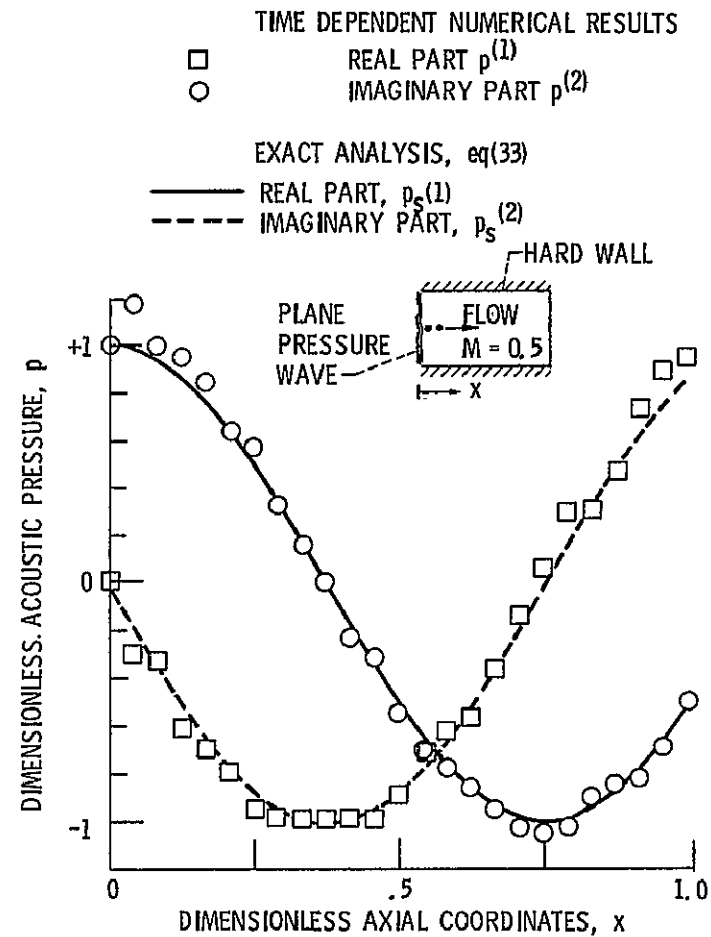


Figure 4 - Analytical and numerical pressure profiles for one-dimensional plane wave sound propagation in a hard wall duct for $M = +0.5$, $\eta = 1$, and $L^*/H^* = 1$ ($I = 25$, $J = 10$, $\Delta t = 0.002438$).

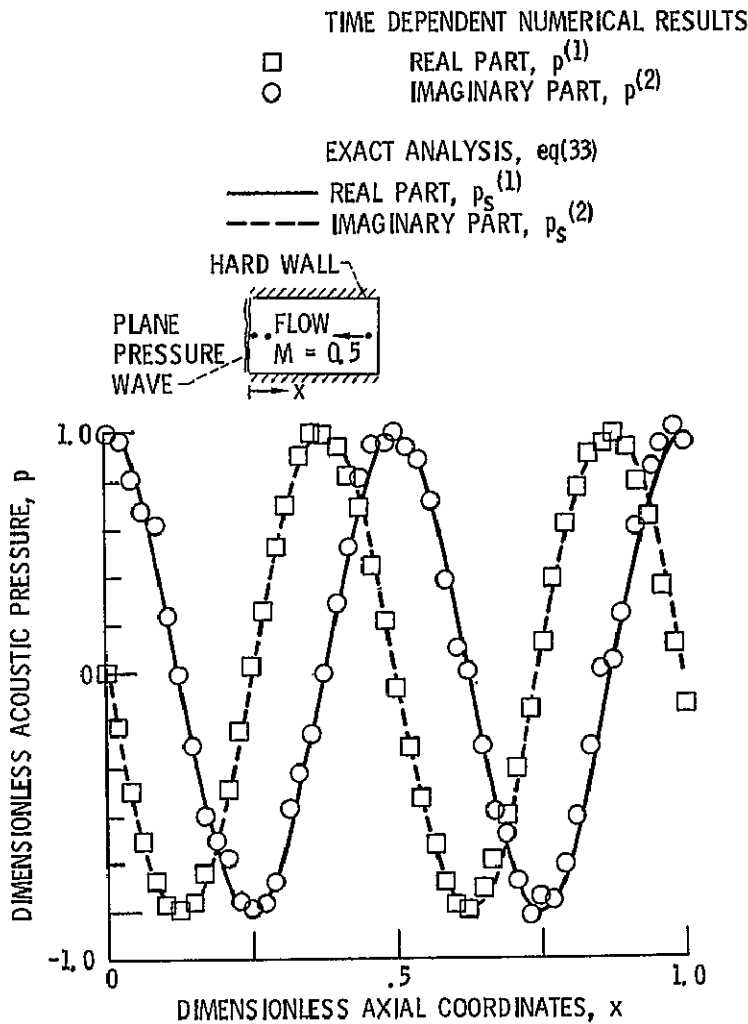


Figure 5. - Analytical and numerical pressure profiles for one-dimensional plane wave sound propagation in a hard wall duct for $M = 0.5$, $\eta = 1$, and $L^*/H^* = 1$ ($I = 49$, $J = 10$, $\Delta t = 0.00064$).

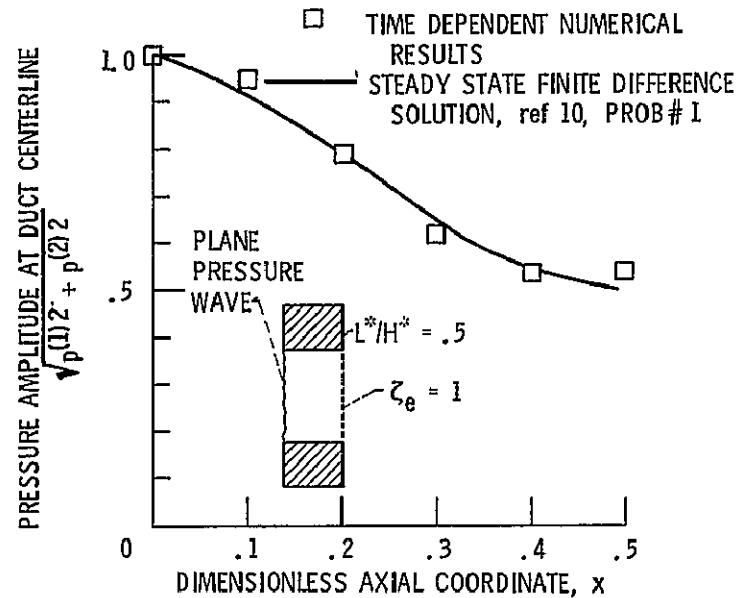


Figure 6. - Pressure magnitude on the duct axis for incident plane wave sound propagation in a soft wall duct ($M = 0$, $\eta = 0.6$, $L^*/H^* = 0.5$, $\zeta = 0.16 - i0.34$, $I = 6$, $J = 10$, $\Delta t = 0.0056$).

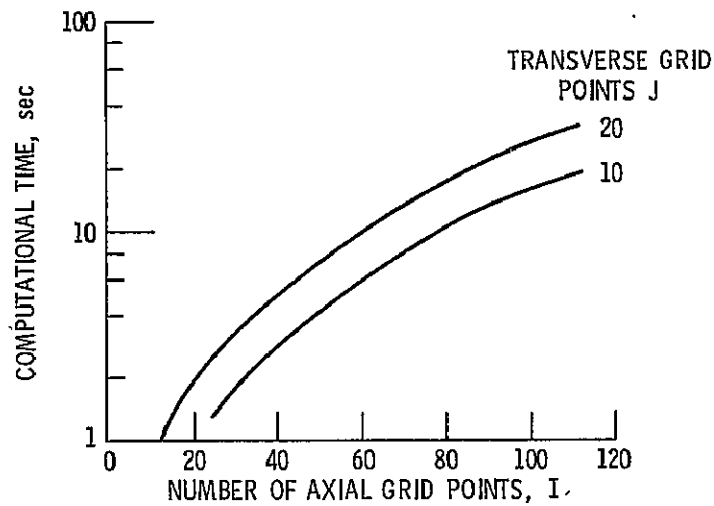


Figure 7. - Effect of increasing number of grid points on calculational time of transient solution for plane wave propagation in a hard wall duct ($M = 0$, $\eta = 1$, $L^*/H^* = 1$, and $\alpha = 1$).

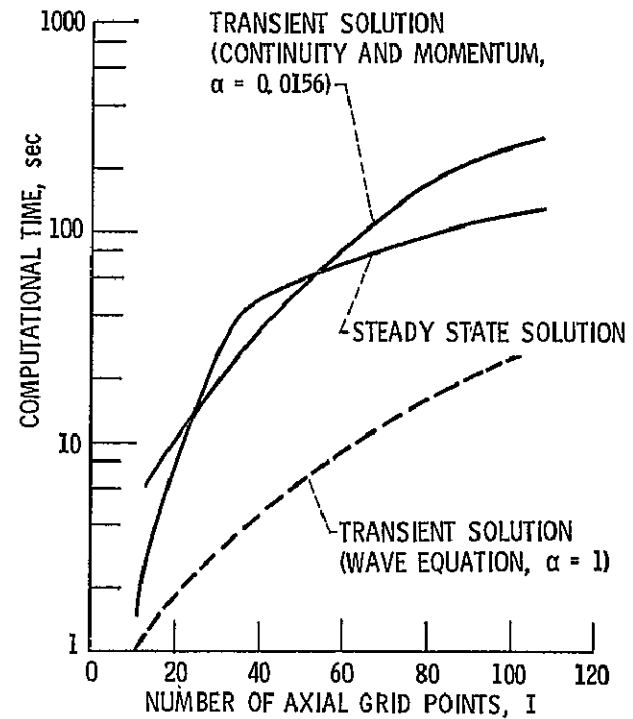


Figure 8. - Comparison of transient and steady state calculations for plane wave propagation in a hard wall duct ($M = 0$, $\eta = 1$, $L^*/H^* = 1$, $J = 20$).

1 Report No NASA TM-79302	2 Government Accession No.	3 Recipient's Catalog No	
4 Title and Subtitle A TIME DEPENDENT DIFFERENCE THEORY FOR SOUND PROPAGATION IN DUCTS WITH FLOW		5. Report Date	
		6 Performing Organization Code	
7 Author(s) K. J. Baumeister		8 Performing Organization Report No E-254	
		10 Work Unit No	
9. Performing Organization Name and Address National Aeronautics and Space Administration Lewis Research Center Cleveland, Ohio 44135		11. Contract or Grant No	
		13 Type of Report and Period Covered Technical Memorandum	
12. Sponsoring Agency Name and Address National Aeronautics and Space Administration Washington, D. C. 20546		14 Sponsoring Agency Code	
15. Supplementary Notes			
16 Abstract A time dependent numerical solution of the linearized continuity and momentum equation is developed for sound propagation in a two-dimensional straight hard or soft wall duct with a sheared mean flow. The time dependent governing acoustic-difference equations and boundary conditions are developed along with a numerical determination of the maximum stable time increments. The analysis begins with a harmonic noise source radiating into a quiescent duct. This explicit iteration method then calculates stepwise in real time to obtain the transient as well as the "steady" state solution of the acoustic field. Example calculations are presented for sound propagation in hard and soft wall ducts, with no flow and with plug flow. Although the problem with sheared flow has been formulated and programmed, sample calculations have not yet been examined. So far, the time dependent finite difference analysis has been found to be superior to the steady state finite difference and finite element techniques because of shorter solution times and the elimination of large matrix storage requirements.			
17. Key Words (Suggested by Author(s)) Finite difference Time dependent Linear acoustics		18. Distribution Statement Unclassified - unlimited STAR Category 71	
19. Security Classif. (of this report) Unclassified	20 Security Classif. (of this page) Unclassified	21. No of Pages	22. Price*

National Aeronautics and
Space Administration

Washington, D.C.
20546

Official Business

Penalty for Private Use, \$300

SPECIAL FOURTH CLASS MAIL
BOOK

Postage and Fees Paid
National Aeronautics and
Space Administration
NASA-451



NASA

POSTMASTER: If Undeliverable (Section 158
Postal Manual) Do Not Return